Effect of Structural Relaxation at Physiological Temperature on the Mechanical Property of Poly(L-lactic acid) Studied by Microhardness Measurements

Yaming Wang,[1,2] **João F. Mano**[1,2]

[1]3B's Research Group –Biomaterials, Biodegradables and Biomimetics, University of Minho, Campus de Gualtar, 4710–057 Braga, Portugal
[2]Polymer Engineering Department, University of Minho, Campus de Azurém, 4800–058 Guimarães, Portugal

ABSTRACT: Besides hydrolysis, the physical properties of poly(L-lactic acid), PLLA, may change, at a shorter timescale, at physiological temperature, because of structural relaxation. This process may be relevant as it may contribute for the time-dependent modifications of the mechanical performance of PLLA-based implants, or in other properties such as specific volume or permeability. In this work, microhardness was measured at room temperature after ageing poly(L-lactic acid) samples at 37°C during different periods, ranging from 15 min to 15 days. For the PLLA analyzed, the initial Vickers microhardness was around 140 MPa and an increase higher than 55% was observed in a time span of 15 days. The relaxation of enthalpy at 37°C was also monitored by differential scanning calorimetry, and both results were successfully described by a simple model that considers a nonexponential evolution of the quantities sensitive to physical ageing. The time-scales of the structural relaxation probed by microhardness or by enthalpy were different, and the results suggested that the evolution of the mechanical property was slower than the later. © 2006 Wiley Periodicals, Inc. J Appl Polym Sci 100: 2628–2633, 2006

Key words: polyesters; biomaterials; biodegradable; glass transition; mechanical properties

INTRODUCTION

Poly(L-lactic acid), PLLA, has been one of the most used biodegradable polymers in a variety of biomedical applications, including in sutures, orthopedic devices, 3-D scaffolds for tissue engineering, and in controlled drug delivery devices.[1–4] The hydrolytic degradation of PLLA during implantation will be accompanied by a change of the physical properties of the material. The continuous decrease of the mechanical properties is particularly relevant for orthopedic applications, where it should be compensated by the remodeling of bone.

The glass transition temperature, T_g, of PLLA ranges typically from 55 to 70°C and, thus, the amorphous fraction will be in a metastable glassy state at physiological temperatures. It is well known that significant variations may be found in the glassy state, if the temperature is not too far below T_g, as a result of the slow changes in molecular configuration, due to the thermodynamic excesses of volume, enthalpy, or entropy, towards its appropriate equilibrium state.

Those can also include changes in the mechanical response, such as creep or stress relaxation. The process of structural relaxation, or physical ageing, involves no change at the chemical point of view, being a reversible physical process.[5–8] The full knowledge of the time-dependent material properties is advantageous if optimum material performance is required. The molecular mechanisms involved in the structural relaxation are not still completely understood, but an acceptable hypothesis would involve the reduction of excess free volume though localized conformational motions leading to the decrease of the fraction of bond with high-energetic conformational energies, such as *gauche*. Therefore, besides chemical degradation, structural relaxation must contribute for the change of the properties of PLLA during implantation. Only a few qualitative studies have been published on structural relaxation in PLLA,[9,10] but this issue was never properly related, to our knowledge, with the change in the mechanical performance during its clinical use.

The most used technique to follow structural relaxation has been differential scanning calorimetry, DSC, that allows to follow the enthalpy loss during ageing.[7,11] Also dilatometric measurements have been often used to probe physical ageing.[6,12] Figure 1 shows a schematic of the dependence of enthalpy and volume on temperature around T_g, including the effect of
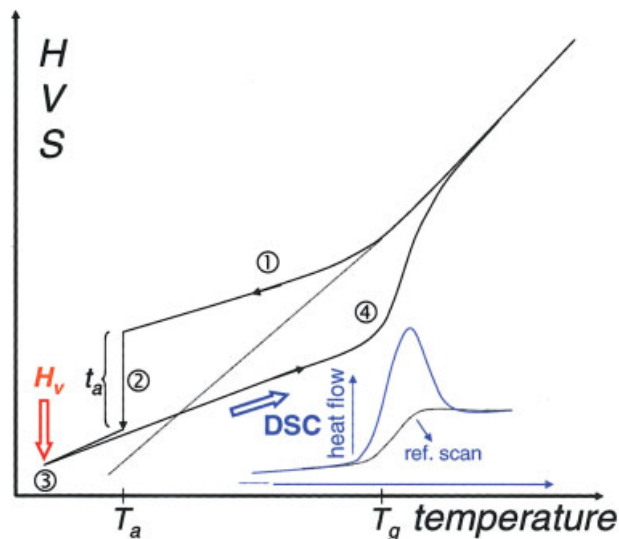
Figure 1 Scheme showing the evolution of primary thermodynamic quantities with the thermal history around the glass transition temperature, T_g, undergone by the samples in this work. The sample is quenched from a temperature above T_g down to the ageing temperature T_a = 37 °C (line 1); after a stage during t_a (line 2) the sample is quenched down to room temperature (line 3). For the DSC experiments, the heat flux is monitored during heating (line 4). The inset graphics shows an example of typical DSC curves obtained during heating for an annealed sample (solid line) and a nonannealed sample (i.e., t_a = 0). For the microhardness experiments, the samples were subjected to the same thermal history up to room temperature, where the microhardness was measured. [Color figure can be viewed in the online issue, which is available at www.interscience.wiley.com.]

the stage at a constant temperature T_a on the evolution of the thermodynamic properties.

In this particular study, we are interested in following the evolution of the mechanical performance of PLLA at 37°C due to physical ageing through microhardness measurements. It has been shown that microhardness in polymeric systems provides indications with practical significance, as well as structural information such as lamellar organization, molecular orientation, and crystallinity.[13–15] Because of its nondestructive character, facility, and quickness, microhardness measurements are a sensitive and adequate method for the investigation of polymers and biomaterials, allowing to obtain information between morphology and macroscopic mechanical properties. Such measurements at the micro- or nanometric level may be also useful when one pretends to map the properties in the surface of heterogeneous systems, including biological tissues. For example, microhardness has been used to access to the spatial monitoring of bone and teeth.[16–22]

Microhardness measurements may be then a useful probe to monitor physical ageing and, at the same time, they provide an adequate approach to follow the

evolution of the mechanical behavior in a clinical situation if the system has been subjected to a previous ageing period at physiological temperature. The number of work reporting the use of microhardness in physical ageing studies is less.[23,24] In this work, the results obtained for PLLA will be compared with DSC to compare the kinetics of structural relaxation probed by these two techniques. This can be included among the wide discussion existing in the literature on the difference in the time scales of relaxation for different properties, where no universal agreement has been found; see, for example, a list of references in refs. 25 and 26.[25,26] In this work, the possibility of inferring the evolution of the mechanical performance of PLLA from DSC data will be then particularly analyzed. However, the main objective of this work is to show and quantify the effect of structural relaxation in the change of the micro-mechanical behavior of PLLA at 37°C.

EXPERIMENTAL

The poly(L-lactic acid) used in this work was the PLA4040 of Cargill-Dow (USA), with 94% L-lactide. The molecular weight, evaluated from GPC was M_n = 69,000 being M_w/M_n = 1.72. PLLA films were prepared by hot-pressing, at 180°C, followed by a quenching in cold water. After erasing the thermal history at 78°C for 5 min, PLA samples were aged at 37°C during different times, in a tube furnace, ranging between 15 min and 15 days.

A Leica VMHT30 equipment was used to measure the microhardness of the samples at room temperature (~21.5°C), using a Vickers diamond pyramid indenter (included angle α = 136°). The microhardness, H_v, was calculated from the residual projected diagonal impression using H_v = 1.854 F/d^2, where d is the mean diagonal length of the indentation in mm and F the applied force in N. A load of 4.9 N was applied for 5 s, to minimize the creep effect. The length of the resulting indentation was measured immediately after load release to avoid complications associated with viscoelastic recovery. Nevertheless, previous dynamic mechanical analysis measurements indicated that the material is essentially elastic at room temperature, exhibiting low damping capability. For each ageing time, the average microhardness was obtained from 10 measurements at randomly selected locations in the sample.

Parallel DSC studies were carried out using a Perkin–Elmer DSC7 equipment. Both temperature and heat flow were calibrated from the melting peak of indium recorded at 10°C min^{-1}. Scans at 10°C min^{-1}, from 30°C to 80°C were performed on the same samples analyzed by microhardness. To obtain an accurate baseline for analyzing the enthalpy recovery data, a second scan was immediately performed at 10°C
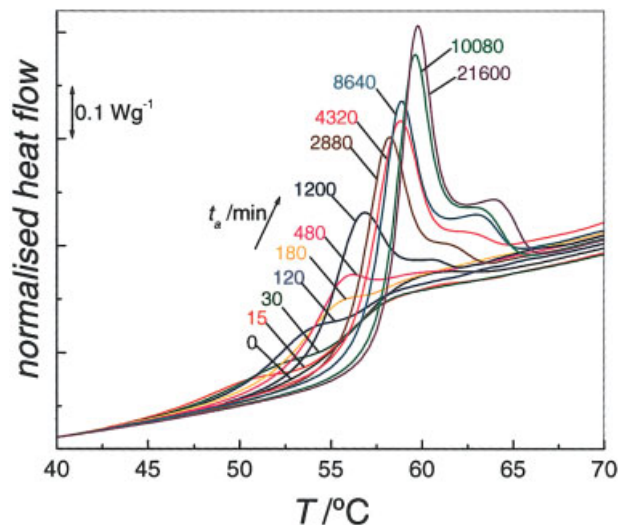
Figure 2 DSC experiments carried out at 10°C min⁻¹ on the studied PLLA samples subjected to a previous annealing at 37°C during different annealing times, t_a, shown in the graphics. [Color figure can be viewed in the online issue, which is available at www.interscience.wiley.com.]

min⁻¹ after quenching the sample to 30°C after the first run, at ~100°C min⁻¹, to register the DSC curve of the unaged sample. As the two curves are obtained one after the other there is expected to be no effect of instrument baseline drift on the calculation of the enthalpy recovery. For a given experiment, the change in enthalpy during physical ageing, ΔH, was determined by the area under the curve obtained by the difference between the aged and unaged scans (see later in the text). The integration was carried out between temperatures where the two curves overlapped, below and above the ageing peak.

RESULTS AND DISCUSSION

Figure 2 shows the evolution of the DSC scans after ageing the sample at 37°C during different times, t_a. As expected, the area of the endothermic peak of the normalized heat flow curves increases with t_a, due to the increase of enthalpy recovery at $T_a = 37$°C. Moreover, the peak position shifts to higher temperatures, as the molecular mobility is reduced during ageing, as a consequence of the reduction of the free volume, being necessary to heat up to higher temperatures so the conformational mobility may take place. Especially for higher t_a, a shoulder is seen in the high-temperature side of the main endothermic peak. This may be an indication that some extent of residual crystallinity may exist in the material, developed during sample preparation, despite the crystallization kinetics of PLLA being intrinsically slow.[27–29] An argument for this observation is the presence of two endothermic peaks, separated by ~5°C, for semicrystalline

PLLA: the low temperature one corresponds to the segmental dynamics of the bulk-like chains and the high temperature one is assigned to the (constrained) conformational mobility of the amorphous chains located within the crystalline structure.[30] In this work the global structural relaxation of the material will be analyzed and thus we will consider the molecular motions of both bulk-like and constrained chains.

There are several models that enable to describe the underlying structural relaxation process from experimental DSC results obtained after different thermal histories. Most of them are multi-parameter phenomenological models, including the Tool–Narayanaswamy–Moynihan,[31–33] Scherer–Hodge,[34–35] Kovacs–Aklonis–Hutchinson–Ramos,[36] and the Gómez–Monleón[37] models. A different and more simple approach was introduced by Cowie and Ferguson,[38,39] which attempts to predict the enthalpy lost on annealing to equilibrium, $\Delta H_\infty(T_a)$, by curve-fitting to the experimental enthalpy data obtained at different ageing times and temperatures, $\Delta H(T_a, t_a)$. The Cowie–Ferguson model considers that, at a given ageing temperature, $\Delta H(T_a, t_a)$ is a self-retarding phenomenon with a simple dependence with time. The progress of the system towards equilibrium is described by the function $\Phi(t) = [H(t) - H_\infty]/[H_0 - H_\infty]$, where H_0, $H(t)$, and H_∞ are the initial, time $= t$, and equilibrium enthalpy values, respectively. The isothermal evolution of $\Phi(t)$ can be expressed by the following empirical equation:

$$\Delta H(T_a, t_a) = \Delta H_\infty(T_a)[1 - \Phi(t_a)] \qquad (1)$$

where ΔH_∞ represents the equilibrium enthalpy of relaxation at $t_a \rightarrow \infty$. The extent of relaxation, $\Phi(t)$, takes usually a stretched exponential form, given by the so-called KWW equation:[40]

$$\Phi(t_a) = \exp[-(t_a/\tau)^{\beta_{KWW}}] \qquad (2)$$

where τ is the characteristic relaxation time such that $\Phi(t_a) = 1/e$ and β_{KWW} ($0 < \beta_{KWW} \leq 1$) is a parameter that indicates the deviation from a pure exponential behavior: $\beta_{KWW} = 1$. It must be noticed that the Cowie–Ferguson model takes into account the nonexponential character of the glass transition dynamics, but not the nonlinearity of structural relaxation, where τ should change as ageing proceeds. Therefore, one should not try to conclude too much from the absolute values extracted; this model must be considered here as a tool to perform an empirical fit and have a relative perception of the relaxation kinetics.

The enthalpy loss between the aged and unaged states at 37°C, $\Delta H(37$°C, $t_a)$, was calculated by applying the following expression:
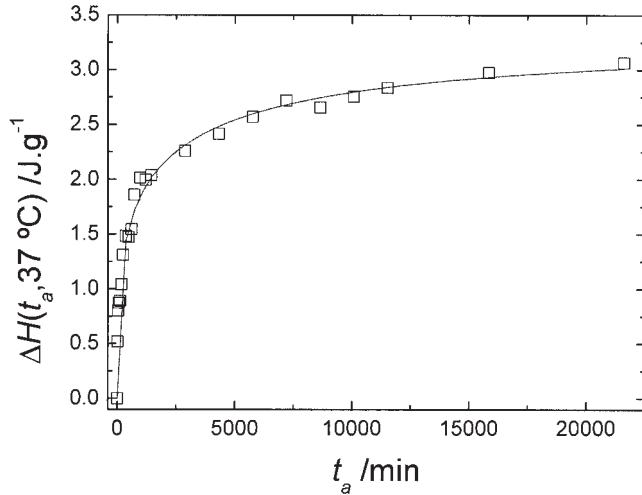
Figure 3 Enthalpy relaxation at 37°C as a function of annealing time (squares). The solid line is the fit according to the Cowie–Ferguson model.
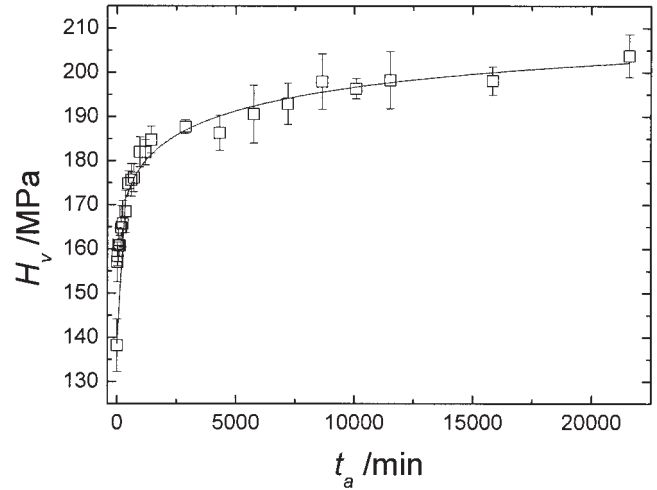

Figure 4 Evolution of microhardness at room temperature for samples previously annealed at 37°C, as a function of the annealing time (squares: mean ± SD, $n = 10$). The solid line is the fit according to the Cowie–Ferguson model.

$$\Delta H(37°C, t_a) = \int_{T_1}^{T_2} (C_{pa}(T) - C_{pr}(T))dT$$

$$= \frac{1}{q^+m} \int_{T_1}^{T_2} \left(\frac{dQ_a(T)}{dt} - \frac{dQ_r(T)}{dt}\right)dT \quad (3)$$

where $C_{pa}(T) - C_{pr}(T)$ is the difference between the experimental heat capacities of the aged and the unaged (reference) sample. The integral is evaluated between T_1, a temperature low enough in the glassy state and a convenient temperature limit T_2 above T_g, in the equilibrium phase. $C_{pa}(T) - C_{pr}(T)$ can be obtained from the heat flux measured in the aged sample, dQ_a/dt, and the heat flux of the reference sample (unaged, i.e., $t_a = 0$), dQ_r/dt, correcting for the heating rate, q^+, and the mass, m, as it is shown in eq. (3).

The values of $\Delta H(37°C, t_a)$ were obtained from the data of Figure 2, using eq. (3) (symbols in Fig. 3). The solid line of Figure 3 is the nonlinear least squares fit of the $\Delta H(37°C, t_a)$ versus t_a data using eqs. (1) and (2) and the Levenberg–Marquhardt algorithm. A good fitting was obtained ($R^2 = 0.99$), with $\Delta H_\infty = 3.26$ J g^{-1} and the KWW parameters shown in Table I. Obviously, ΔH_∞ at 37°C should be highly dependent on the crystallinity degree: we expect that this value will be

maximum for a full amorphous material, because $\Delta C_p(T_g)$ is maximum in this case and $\Delta H_\infty \approx (T_g - T_a) \Delta C_p(T_g)$.

Parallel studies on PLLA have been performed to elucidate on the glass transition dynamics, from DSC experiments on samples after being subjected to different thermal histories below T_g.[41] The data was treated using a physical model based on the concept of configuration entropy[37] and it was possible to extract information on the temperature evolution of the characteristic times and on the β_{KWW} parameter. Interestingly, it was obtained $\beta_{KWW} = 0.40$ for a nearly amorphous PLLA[41] that is close to what was obtained in this work using the Cowie–Ferguson model on the DSC data (Table I).

The KWW equation also enables to correlate the data with the existence of a distribution of characteristic times, where β_{KWW} quantifies the broadness of the spectrum: small values of β_{KWW} imply a broad distribution and a single time is reached when $\beta_{KWW} = 1$. An average relaxation time $\langle\tau\rangle$ for the distribution may be estimated using

$$\langle\tau\rangle = \tau\Gamma(1 + 1/\beta_{KWW}) \quad (4)$$

where Γ is the gamma function. The average relaxation time for enthalpy recovery is shown in Table I.

A similar data treatment was also performed with the microhardness measurements at 37°C after different ageing times (Fig. 4). Values between 130 and 210 MPa were obtained, being typical for amorphous polyesters.[15] The magnitude of H_v at short loading times correlates, in a macroscopic viewpoint, with the yield stress and the modulus of the material; it was shown that a number of parameters, such as Young's

TABLE I
Structural Relaxation Parameters at 37°C Probed by Enthalpy Recovery (ΔH) and Microhardness (H_v) Using the KWW Model

	τ/min	β_{KWW}	log ($\langle\tau\rangle$/min)
ΔH	1600	0.37	3.83
H_v	3260	0.28	4.62

modulus, shear viscosity, creep exponent, and activation energy for flow can be estimated from the analysis of Vickers micro-indentation profile by means of atomic force microscopy.[42] On the other hand, H_v is related to the critical stresses required for irreversible deformation of solidified molecular aggregates (e.g., crystalline lamellae or microfibrils), thus being a bridge between bulk and microstructural quantities.[13–15,43] In a biomedical point of view, microhardness measurements have been often used to probe changes in the mechanical behavior of bone and biomaterials. For example, microhardness shows correlation with fracture toughness in bone of baboons with different ages.[44] It was also showed that microhardness measurements could be useful and effective to probe osseointegration of implants.[45,46]

Similarly to the enthalpy change upon ageing, the evolution of microhardness at room temperature, after ageing at T_a, during a time t_a, may be written as

$$H_v(T_a, t_a) = H_{v,0}(T_a) + \Delta H_v(T_a)[1 - \Phi(t_a)] \quad (5)$$

where $H_{v,0}(T_a)$ is the microhardness of the non-aged sample and $\Delta H_v(T_a) = H_{v,\infty}(T_a) - H_{v,0}(T_a)$, being $H_{v,\infty}(T_a)$ the equilibrium microhardness at $t_a \to \infty$. The combination of eqs. (5) and (2) was used to fit the data in Figure 4 (solid line) and the KWW-adjustable parameters are presented in Table I. The fitting also allowed to obtain $H_{v,0}(37°C) = 139$ MPa and $\Delta H_v(37°C) = 78$ MPa. This indicates that microhardness in PLLA may change more than 55%, relatively to the unaged material, just as the results of physical ageing; note that within the ageing times analyzed no significant changes occurred in the thermal properties of PLLA because of chemical degradation, as the second scans (unaged samples) were very similar for all samples analyzed. In a practical point of view, such results provide evidences for a significant change in the mechanical behavior due to structural relaxation at body temperature, that may be reflected in the general performance of an implanted PLLA-based material, especially in the first weeks (see estimation of the time scale of the relaxation in Table I). Note that the time scale of physical aging is much shorter than the conventional chemical degradation. It was reported that amorphous PLLA specimens retained mechanical properties for longer time than did semicrystalline PLLA.[47] Amorphous PLLA would exhibit mechanical stability for up to 12 weeks *in vivo*.[48]

The estimated characteristic times for structural relaxation are different when probed by calorimetric or microhardness measurements (Table I). This is also reflected in the differences on the average value for the distribution of relaxation times, $\langle \tau \rangle$. It would be suitable to predict the evolution of mechanical properties from DSC data, as the protocols and data treatments assigned to this technique are well established; more-

over, the temperature control in DSC is excellent and one may work with small amounts of samples. However, it has been demonstrated that the direct comparison between relaxing properties is not trivial, notwithstanding that the results result from the same molecular mechanism;[49] as commented by Echeverría et al., we may detect even contradictions, with some researchers finding that the time scales are the same for different properties, where some other groups show that they differ.[26]

For example, for poly(methyl methacrylate), poly-(styrene-*co*-acrylonitrile) and their blends, the relaxation times obtained from enthalpy recovery and viscoelastic measurements showed a similar dependence on the ageing conditions.[50] For polyetherimide, the time scales to reach equilibrium for enthalpy and mechanical measurements (creep) were also found to be the same, within experimental error.[51] However, for poly(vinyl acetate), it was found that the mechanical properties, probed by shear stress relaxation, reach equilibrium before either volume or enthalpy;[52] also from dynamic mechanical analysis, following the loss factor, it was found that the evolution of the mechanical behavior is faster than the enthalpy recovery in poly(methyl methacrylate).[53] In other situations, opposite conclusions were achieved: in poly(vinyl acetate), the equilibrium relaxation times were found to be smaller from enthalpy results an largest from dynamic mechanical analysis;[54] in polystyrene it was found that enthalpy recovery is faster than creep evolution by about an order of magnitude;[55] for low molecular glasses, it was found, for the case of amorphous selenium, that below T_g the time for reaching the equilibrium is shorter for enthalpy than for creep.[26] The results in the present work seem to be in accordance with the last group of findings where the evolution of the mechanical properties, monitored by microhardness, is slower than the relaxation of enthalpy.

The stretch exponent, β_{KWW} is also different for the two physical probes, suggesting a broad spectrum of relaxation times for microhardness measurements. Cowie et al. also reported different values of β_{KWW} for enthalpy and volume ageing.[49] This finding demonstrates that the structural changes upon physical ageing reflects differently on the properties "enthalpy" and "microhardness." As suggested by Echeverría et al.,[26] based on the work of Thurau and Ediger,[56] the differences in the time scales observed in macromolecular properties could be assigned to divergences of time scales for rotational and translational diffusion due to the presence of dynamic special heterogeneities at a molecular level. It is thus not straightforward the direct relationship between the kinetics of structural relaxation measured by different physical properties.

CONCLUSIONS

It was shown that microhardness in low crystalline PLLA changes significantly at 37°C due to physical ageing: for the material analyzed, an increase above 55% may be observed in a time span of 15 days. This may have implications in the mechanical performance of amorphous PLLA-based implants *in vivo*, besides the conventional chemical degradation, that take place in a much longer time-scale. Besides the mechanical properties, we expect that volume should change, although in a low extent, with ageing time at 37°C, which may be also relevant in some situations where the geometry of the implant must be precise. The studies in this work were performed in PLLA, but physical ageing should also be present in any glassy material exhibiting a glass transition temperature not far above body temperature, such as poly(DL-lactide) or copolymers of L-lactide and glycolic acid. It was also possible to monitor the evolution of structural relaxation of PLLA by DSC, and it was found that the time scales of the evolution for microhardness and for enthalpy are not coincident.

References

1. Thomson, R. C.; Wake M. C.; Yaszemski M. J.; Mikos, A. G. Adv Polym Sci 1995, 122, 245.
2. Agrawal, C. M.; Ray, R. B. J Biomed Mater Res 2001, 55, 141.
3. Södegard, A.; Stolt, M. Prog Polym Sci 2002, 27, 1123.
4. Kim, H. D.; Bae, E. H.; Kwon, I. C.; Pal, R. R.; Nam, J. D.; Lee, D. S. Biomaterials 2004, 25, 2319.
5. Struick, L. C. E. Physical Aging in Amorphous Polymers and Other Materials; Elsevier: New York, 1978.
6. Kovacs, A. J. Adv Polym Sci 1963, 3, 394.
7. Hodge, I. M. J Non-Cryst Solids 1994, 169, 211.
8. Hutchinson, J. M. Prog Polym Sci 1995, 20, 703.
9. Celli, A.; Scandola, M. Polymer 1992, 33, 2699.
10. Teramoto, Y.; Nishio, Y. Biomacromolecules 2004, 5, 397.
11. Hodge, I. M. Science 1995, 267, 1945.
12. Kovacs, A. J. Polym Sci 1958, 30, 131.
13. Baltá Calleja, F. J. Trends Polym Sci 1994, 2, 419.
14. Baltá Calleja, F. J.; Fakirov, S. Trends Polym Sci 1997, 5, 246.
15. Baltá Calleja, F. J.; Fakirov, S. Microhardness of Polymers; Cambridge University Press: Cambridge, 2000.
16. Evans, G. P.; Behiri, J. C.; Currey, J. D.; Bonfield, W. J Mater Sci Mater M 1990, 1, 38.
17. Ziv, V.; Wagner, H. D.; Weiner, S. Bone 1996, 18, 417.
18. Riches, P. E.; Everitt, N. M.; Heggie, A. R.; McNally, D. S. J Biomech 1997, 30, 1059.
19. Hengsberger, S.; Kulik, A.; Zysset, P. Bone 2002, 30, 178.
20. Bushby, A. J.; Ferguson, V. L.; Boyde, A. J Mater Res 2004, 19, 249.
21. Meredith, N.; Sherriff, M.; Setchell, D. J.; Swanson, S. A. V Arch Oral Biol 1996, 41, 539.
22. Wang, R. Z.; Weiner, S. Connect Tissue Res 1998, 39, 269.
23. Ania, F.; Martinezsalazar, J.; Calleja, F. J. B. J Mater Sci 1989, 24, 2934.
24. Pérez, E.; Pereña, J. M.; Benavente, R.; Bello, A.; Lorenzo, V. Polym Bull 1992, 29, 233.
25. Simon, S. L.; Plazek, D. J.; Sobieski, J. W.; McGregor, E. T. J Polym Sci Part B: Pol Phys 1997, 35, 929.
26. Echeverría, I.; Kolek, P. L.; Plazek, D. J.; Simon, S. L. J. Non-Cryst Solids 2003, 324, 242.
27. Iannace, S.; Nicolais, L. J Appl Polym Sci 1997, 64, 911.
28. Miyata, T.; Masuko, T. Polymer 1998, 39, 5515.
29. Di Lorenzo, M. L. Polymer 2001, 42, 9441.
30. Wang, Y.; Gómez Ribelles, J. L.; Salmerón Sánchez, M.; Mano, J. F. Macromolecules 2005, 38, 4712.
31. Tool, A. Q. J Am Ceram Soc 1946, 29, 240.
32. Narayanaswamy, O. S. J Am Ceram Soc 1971, 54, 491.
33. Moynihan, C. T.; Easteal, A. J.; DeBolt, M. A.; Tucker, J. J Am Ceram Soc 1976, 59, 12.
34. Scherer, G. W. J Am Ceram Soc 1984, 67, 504.
35. Hodge, I. M. Macromolecules 1987, 20, 2897.
36. Kovacs, A. J.; Aklonis, J. J.; Hutchinson, J. M.; Ramos, A. R. J Polym Sci Part B: Pol Phys 1979, 17, 1097.
37. Gómez Ribelles, J. L.; Monleón Pradas, M. Macromolecules 1995, 28, 5867.
38. Cowie, J. M. G.; Ferguson, R. Polym Commun 1986, 27, 258.
39. Cowie, J. M. G.; Ferguson, R. Macromolecules 1989, 22, 2307.
40. Williams, G.; Watts, D. C. Trans Faraday Soc 1970, 66, 80.
41. Mano, J. F.; Gómez Ribelles, J. L.; Alves, N. M.; Salmerón Sanchez, M. Polymer 2005, 46, 8258.
42. Rouxel, T.; Sangleboeuf, J.-C.; Moysan, C.; Truffin, B. J Non-Cryst Solids 2004, 344, 26.
43. Santa Cruz, C.; Baltá Calleja, F. J.; Zachmann, H. G.; Stribeck, N.; Asano, T. J Polym Sci Part B: Pol Phys 1991, 29, 819.
44. Wang, X. D.; Masilamani, N. S.; Mabrey, J. D.; Alder, M. E.; Agrawal, C. M. Bone 1998, 23, 67.
45. Fini, M.; Giavaresi, G.; Greggi, T.; Martín, L.; Aldini, N. N.; Parisini, P.; Giardino, R. J Biomed Mater Res 2003, 66A, 176.
46. Giavaresi, G.; Fini, M.; Cigada, A.; Chiesa, R.; Rondelli, G.; Rimondini, L.; Aldini, N. N.; Martín, L.; Giardino, R. J Biomed Mater Res 2003, 67A, 112.
47. Li, S. M.; Grreau, A.; Vert, M. J Mater Sci Mater M 1990, 1, 198.
48. Pistner, H.; Stallforth, H.; Gutwald, R.; Muhling, J.; Reuther, J.; Michel, C. Biomaterials 1994, 15, 439.
49. Cowie, J. M. G.; Harris, S.; McEwen, I. J. Macromolecules 1998, 31, 2611.
50. Mijovic, J.; Ho, T. Polymer 1993, 34, 3865.
51. Echeverria, I.; Su, P.-C.; Simon, S. L.; Plazek, D. J. J Polym Sci Part B: Pol Phys 1995, 33, 2457.
52. Cowie, J. M. G.; Ferguson, R.; Harris, S.; McEwen, I. J. Polymer 1998, 39, 4393.
53. Perez, J.; Cavaille, J. Y.; Calleja, R. D.; Ribelles, J. L. G.; Pradas, M. M.; Greus, A. R. Makromol Chem Macromol Chem Phys 1991, 192, 2141.
54. Sasabe, H.; Moynihan, C. T. J Polym Sci Part B: Pol Phys 1978, 16, 1447.
55. Roe, R. J.; Millman, G. M. Polym Eng Sci 1983, 23, 318.
56. Thurau, C. T.; Ediger, M. D. J Chem Phys 2002, 116, 9089.